Design and Analysis of TQS01, a 90 mm Nb$_3$Sn Model Quadrupole for LHC Luminosity Upgrade Based on a Key and Bladder Assembly

S. Caspi, G. Ambrosio, N. Andreev, E. Barzi, R. C. Bossert, D. R. Dietderich, P. Ferracin, A. Ghosh, S. A. Gourlay, A. R. Hafalia, C. R. Hannaford, V. S. Kashikhin, V. V. Kashikhin, A.F. Lietzke, S. Mattafirri, A. D. McInturff, I. V. Novitsky, and G. L. Sabbi, D. Turrioni, R. Yamada, A. V. Zlobin

Abstract—**The US LHC Accelerator Research Program (LARP) is developing Nb$_3$Sn accelerator magnet technology for the LHC luminosity upgrade. Two 90 mm "Technology Quadrupole" models (TQS01, TQC01) are being developed in close collaboration between LBNL and FNAL, using identical coil design, but two different support structures. The TQS01 structure was developed and tested at LBNL. With this approach coils are supported by an outer aluminum shell and assembled using keys and bladders. In contrast, the second model TQC01, utilize stainless steel collars and a thick stainless steel skin. This paper describes the TQS01 model magnet, its 3D ANSYS stress analysis, and anticipated instrumentation and assembly procedure.**

Index Terms—**LARP, LHC IR, Nb$_3$Sn, quadrupole magnet, bladders, keys.**

I. INTRODUCTION

THE US has taken collaborative R&D steps toward an upgrade of the LHC Interaction Region (IR). Following a series of LHC Accelerator Research Program (LARP) collaboration meetings [1], the three US laboratories (BNL, FNAL, and LBNL) have started a magnet development program towards the fabrication of a full scale IR quadrupole prototype. The expected operational demands (operating gradient >205 T/m, bore >90 mm, excellent field quality, and high radiation loads) require the use of Nb$_3$Sn superconducting cable. Immobilizing the conductor against substantial Lorentz stress (120 MPa), without degrading the conductor, yielded two possible solutions to the magnet structure and assembly: 1) a collar based structure (proposed by FNAL) [2] and 2) a "key and bladder" shell-based structure (Fig. 1) [3-4] The latter approach was successfully used in a number of Nb$_3$Sn magnets at LBNL [5-6]).

The shell-based structure approach uses bladders for precise, low-level pre-stress control, with negligible stress "overshoot" during magnet assembly. Interference keys are inserted to retain the pre-stress and allow bladder removal. A tensioned aluminum shell compresses internal iron and coil components, and causes a substantial fraction of the operational pre-stress to develop during cool-down. Accordingly, the final coil pre-stress is monotonically approached from below, without overstressing the fragile conductor. A satisfactory assembly and cool-down mechanical test of this proposed structure has been reported [7].
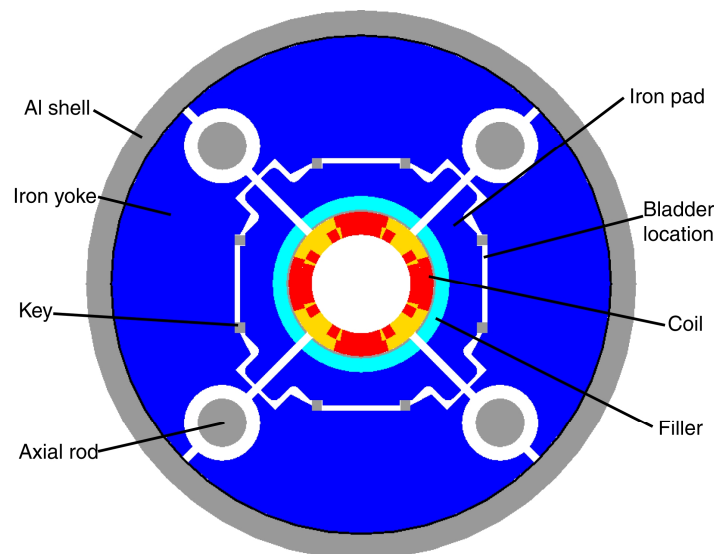
Fig. 1. TQS01 magnet cross-section showing coils, fillers, pads, keys, yokes, skin and axial supporting rods.

TABLE I
MAGNET PARAMETERS

	Unit	Layer 1	Layer 2
STRAND			
Type		MJR	
Diameter	mm	0.7	
Cu/Sc		0.89 ± 0.02	
Assumed J_{ss} (4.2 K, 12 T)	A/mm^2	2100	
CABLE			
N strands		27	
Mid-thickness bare	mm	1.260 ± 0.01	
Width bare	mm	10.025 ± 0.05	
Keystone angle	Degree	1.0 ± 0.1	
Insulation thickness	mm	0.125	
COILS			
Turns per block		6/12	16
Mandrel diameter	mm	90	
STRUCTURE			
Shell thickness	mm	22	
Shell outer diameter	mm	500	
OPERATING EXPECTATIONS at 4.2 K (1.9 K):			
Short sample current	kA	12.45 (13.52)	
Peak conductor field	T	11.20 (12.15)	9.96 (10.8)
G_{ss}	T/m	222 (239)	
Stored energy	kJ/m	392 (456)	
Inductance	mH/m	5	
Coil azimuthal stress	MPa	123 (144)	83 (97)
Fx per quadrant	MN/m	2.97 (3.38)	
Axial force	kN	351 (413)	

II. DESIGN PARAMETERS

A. Status

At present, four 1 meter long, double-layer "practice" coils have been wound, cured, reacted and impregnated (Fig. 2). The coils will be used in a full mechanical test assembly, and subsequently section-cut and analyzed. Winding and curing of the production coils for TQS01 and TQC01 is expected to occur at FNAL, followed by reaction and impregnation at LBNL. The first four final coils are expected to be assembled in TQS01 by the end of 2005, and subsequently tested in early 2006.

B. Cable, Coil Winding and Reaction

The partially keystoned cable was made from 27 Modified Jelly Roll (MJR) Nb$_3$Sn strands with a current density around 2100 A/mm^2 at 12 T, 4.2 K (Table I). The operating gradients are expected to be 222 T/m (4.2 K) and 239 T/m (1.9 K). The coil cross-section (Fig. 3) features a single wedge.

All winding poles, end-spacers and shoes were made of aluminum-bronze and cut by water jet (to match a design profile according to the program BEND). The inner layer is wound and cured with a ceramic binder, creating a solid structural surface upon which the second layer can be wound. A second application of ceramic binder bonds both layers together.

Reaction tooling accommodates two coils at the same time

(Fig. 4, left), reducing the number of final coil reactions from four to two. The reaction schedule is 48 hrs at 210 C followed by 48 hrs at 400 C and a final high temperature phase of 48 hrs at 640 C. Similar potting tooling is available for vacuum-pressure impregnation, after NbTi leads are attached and the coils instrumented with voltage taps and strain gauges.
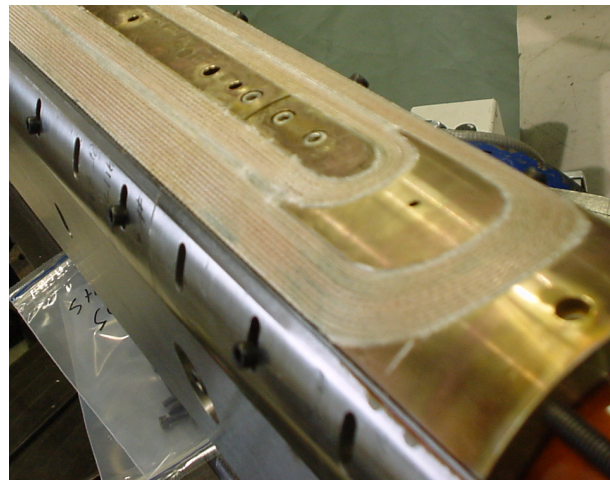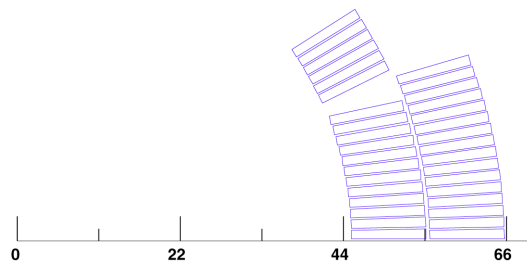

Fig. 2. Practice coil: inner layer.
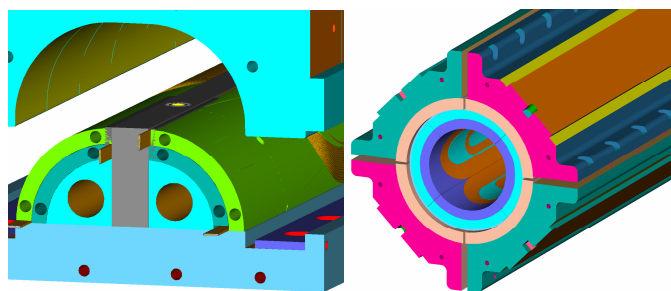

Fig. 3. Coil cross-section (scale in mm).

Fig. 4. The reaction tooling accommodates two double-layers coils (left). After epoxy impregnation, the coils are pre-assembled, with four iron load-pads, into a "coil-pack" (right).

C. Coil-Pack Pre-Assembly

The four coils will be assembled with four iron load pads, which will be bolted together to make the "coil-pack" (Fig. 4-right). The coil-pack assembly includes an iron spacer in the straight section and a stainless steel spacer over the ends that reduces "end" field. The spacers place the coils symmetrically around the bore, and facilitate uniform radial loading along the length of each coil.

D. Structure

The main components of the structure are the four iron yoke-stack quadrants, symmetrically spaced inside a 6061-T6 aluminum cylindrical shell (Fig. 5). Each yoke-stack utilized 10, 50.8 mm thick steel laminations, precision ground and assembled with one tie-rod per quadrant. Each yoke lamination was cut to provide clearance cavities for the coil-pack and four aluminum, axial-loading rods. A 1.6 mm-thick rolled-steel sheet is sandwiched between the shell and the yoke, to simulate a welded enclosure stainless steel vessel that will be expected to serve as an integrated cryostat for the eventual full-length accelerator magnet.

E. "Bladders and Keys" - Final assembly

Four 69.8x1016.0 mm bladders (made of stainless steel sheets, 0.25mm thick) will be pressurized with water acting as internal presses, to stretch the outer aluminum shell and compress the inner coil-pack and yoke assemblies. Keys are to be placed into the clearances between the coil-pads and yoke-blocks, and shimmed to provide the required 300 K pre-stress. After shimming of the keys, the bladders will be removed.

Axial pre-loading of the coil-ends is accomplished with a pressurized piston that tensions the four axial aluminum rods (6061 T6, 44.45 mm diameter). The rods longitudinally compress the coils in between two 89 mm thick stainless steel end-plates (Fig. 6).
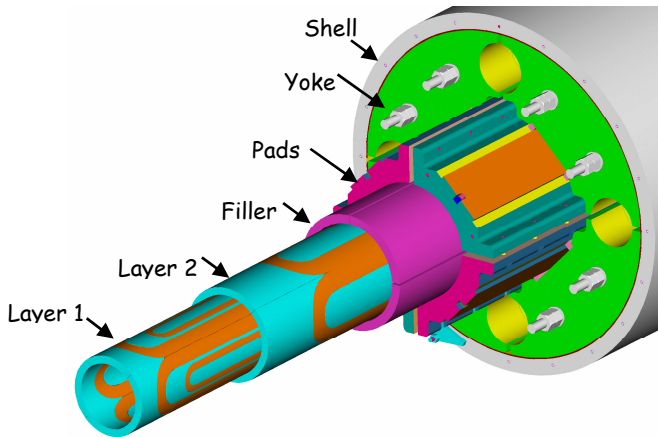
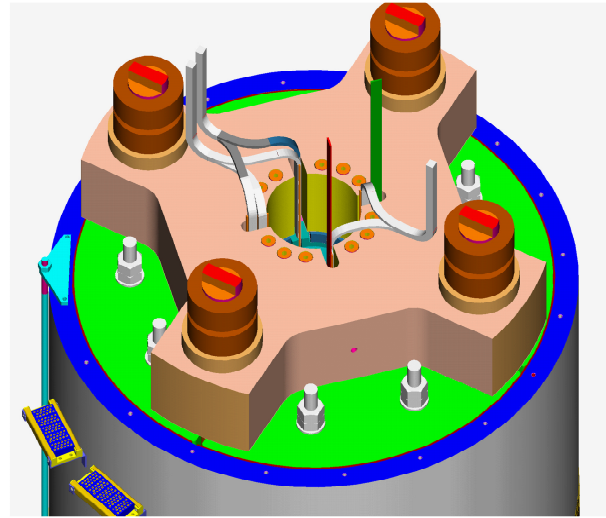

Fig. 5. View of coils and supporting structure.

Fig. 6. Axial end plate and rods.

The assembly process is monitored by strain-gauges on the outer aluminum shell and on the four axial aluminum rods. All pre-loads are planned to be applied in steps, with interference-key thicknesses gradually shimmed one quadrant at a time.

III. ANALYSIS

The magnet design and analysis was completely integrated. The computed (3D) coil geometry was loaded into CAD (ProE) and assembled with the coil-support structure: yoke, shell, end-plates and axial rods. The resulting CAD assembly was then loaded into TOSCA (using the MODELLER interface) and directly into ANSYS (using the ANSYS-ProE interface). The 3D magnetic analysis was used to determine the field in the ends and the conductor Lorentz forces that were subsequently used by ANSYS to estimate the excitation responses of the assembled system [4].

The analysis was done with and without friction ($\mu = 0.2$). to determine the 300K pre-loading that prevents coil-separation azimuthally at the winding-poles, and axially at the coil ends when energized at the anticipated 1.9 K conductor short-sample limit. Several ANSYS iterations resulted in a 300 K magnet assembly sequence which started with a 65 MPa pre-loading of the axial rods ("axial" in Fig. 7, with 4.2 K and 1.9 K short-sample limits indicated by short vertical lines).
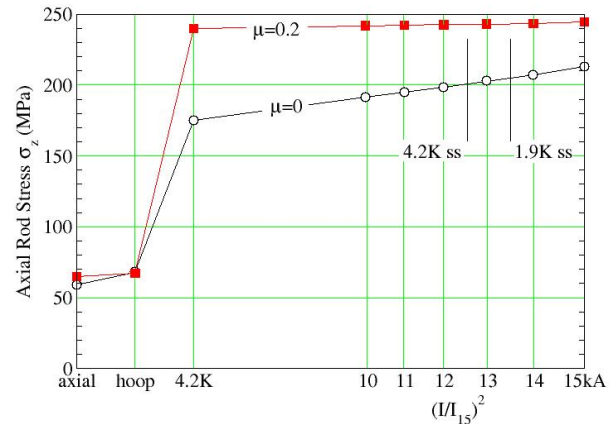
Fig. 7. Computed load sequence for the axial rods. Short vertical lines indicate the anticipated 4.2 K and 1.9 K short-sample limits.
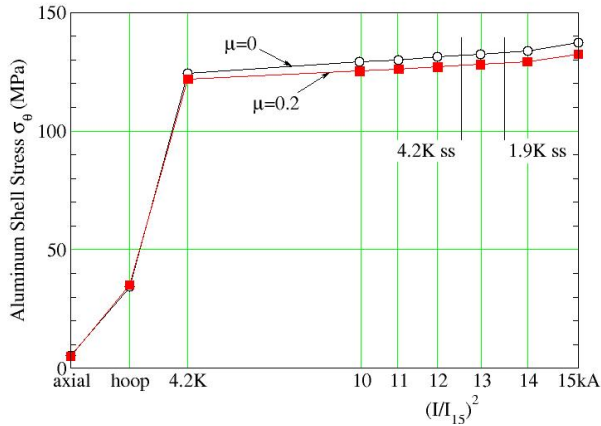
Fig. 8. Computed load sequence for the aluminum shell.

The bladders were subsequently pressurized ("hoop" in Fig. 8) for a shell tension of 35 MPa, after which they were replaced with keys leaving each coil with a low nominal azimuthal stress of 35 MPa in layers 1 and 2 (Fig. 9,10). During cool-down, the shell-stress increases to 120-130 MPa, relatively independent of friction (Fig. 8). At the same time the coils gain ~100 MPa for a final azimuthal compression of 120-140 MPa (depending upon friction).The rod-tension significantly depends upon the assumed friction factor resulting at 175 MPa (without friction), and 240 MPa (with friction). The stress is given at the center of each layer
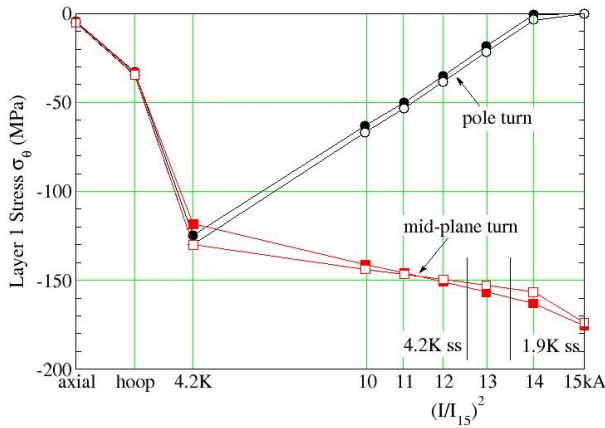
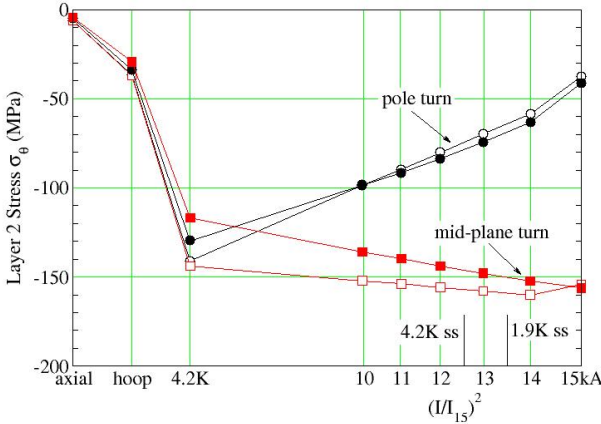Fig. 9. Computed load sequence for layer-1 (open $\mu = 0$, closed $\mu = 0.2$).

Fig. 10. Computed load sequence for layer-2 (open $\mu = 0$, closed $\mu = 0.2$).

During magnet excitation, the Lorentz forces reduce the coil stress in the pole-turn, while increasing it at the mid-plane. Layer-1's pole-turn is expected to completely unload at ~14 kA (Fig. 9), 4% beyond the expected 1.9 K short sample limit. Epoxy impregnation may provide additional margin against coil-pole separation. Meanwhile, at 14 kA layer-2's pole-turn is expected to partially unload to -60 MPa, while the mid-plane compression increases to -155 MPa (depending upon friction assumptions. A detailed 3D mechanical model and analysis of the magnet ends was performed with the goal of computing the pole-turn gaps that could be expected with and without friction. A layer-1 gap is expected to start opening (Fig. 11) at 12 kA (no friction) and 14kA (with friction). A layer-2 gap is expected to start opening (Fig. 12) at 10 kA (no friction) and 11 kA (with friction). In both layers the gap is expected to be less than 20 μm at 14 kA.
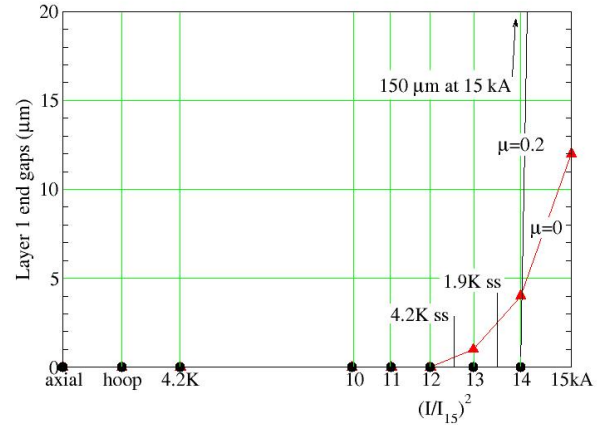
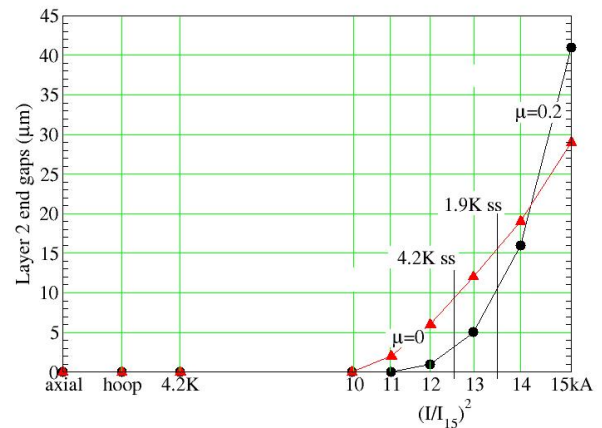Fig. 11. Computed end-gaps between pole and first turn (layer 1).

Fig. 12. Computed end-gaps between pole and first turn (layer 2).

IV. CONCLUSIONS

The design and analysis of the LARP quadrupole magnet TQS01 was presented and discussed. This magnet, expected to be assembled at LBNL by the end of 2005 and tested in early 2006, was designed with an aluminum support structure that is pre-stressed with bladders and keys (azimuthal), and a piston (axial). A 3D magnetic and mechanical analysis was performed to investigate the structural and coil behavior during pre-stressing, cool-down and excitation. This study

predicted no azimuthal separation between coil and pole, with axial gaps at the magnet end below 15 μm at the anticipated 1.9 K short-sample limit.

REFERENCES

[1] LARP website, http://www.agsrhichome.bnl.gov/LARP/.
[2] R. C. Bossert, *et al*., "Development of a 90-mm Nb3Sn Technological Quadrupole for LHC Upgrade based on SS Collar", this conference.
[3] G. Sabbi et al., "Nb3Sn quadrupole magnets for the LHC IR", *IEEE Trans. Appl. Superconduct*., Vol. 13, no. 2, June 2003, pp. 1262-1265.
[4] S. Caspi, *et al*., "Mechanical design of a second generation LHC IR quadrupole", *IEEE Trans. Appl. Superconduct*., Vol. 14, no. 2, June 2004, pp. 235-238.
[5] S. Caspi, *et al*., "The use of pressurized bladders for stress control of superconducting magnets", *IEEE Trans. Appl. Superconduct*., Vol. 11, no. 1, March 2001, pp. 2272-2275.
[6] A. R. Hafalia, *et al*., "A new support structure for high field magnet", *IEEE Trans. Appl. Superconduct*., Vol. 12, no. 1, March 2002, pp. 47-50.
[7] A. R. Hafalia, *et al*., "Structure for an LHC 90 mm Nb_3Sn quadrupole magnet", *IEEE Trans. Appl. Superconduct*., Vol. 15, no. 2, June 2005, pp. 1444-1447.